The Journal of Immunology

RESEARCH ARTICLE | JANUARY 01 2012

# UXT-V1 Facilitates the Formation of MAVS Antiviral Signalosome on Mitochondria FREE

Yuefeng Huang; ... et. al

*J Immunol* (2012) 188 (1): 358–366.
https://doi.org/10.4049/jimmunol.1102079

# UXT-V1 Facilitates the Formation of MAVS Antiviral Signalosome on Mitochondria

**Yuefeng Huang,[1] Heng Liu,[1] Rui Ge, Yi Zhou, Xiwen Lou, and Chen Wang**

**Virus infection induces the MAVS–TNFR-associated factor (TRAF) 3 signaling axis on mitochondria. It remains to elucidate the corresponding regulatory processes. In this study, we identify UXT-V1 as a novel TRAF3-binding protein. UXT-V1 is critical for the virus-induced activation of NF-κB and IFN regulatory factor 3. Reduction of UXT-V1 impairs the induction of IFN-β and attenuates the host antiviral responses. The N-terminal TRAF-binding motif of UXT-V1 binds to the C-terminal TRAF domain of TRAF3, thus facilitating the interaction between TRAF3 and MAVS. Notably, TRAF3 and TNFR-associated death domain protein are recruited onto mitochondria upon virus infection. These translocations are blocked when knocking down UXT-V1. Thus, UXT-V1 represents a novel integral component of the MAVS signalosome on mitochondria, mediating the innate antiviral signal transduction.** ***The Journal of Immunology*****, 2012, 188: 358–366.**

To initiate robust antiviral responses, the immune system must recognize pathogen-associated molecular patterns effectively (1, 2).The first family of pattern recognition receptor molecules identified is the TLRs, in which TLR3, TLR7/TLR8, and TLR9 are capable of detecting viral nucleic acids (3, 4). In contrast to TLRs that monitor the presence of topologically extracellular viruses in immune cells, RIG-I and MDA5 have been characterized as ubiquitous sensors for detecting cytosolic RNA viruses during primary responses of host cells (5–7).

Once RIG-I/MDA5 senses viral RNAs, a mitochondrial signalosome is formed, which includes MAVS (also known as IPS1, VISA, and Cardif), TNFR-associated factor (TRAF) 3, TNFR-associated death domain protein (TRADD), and so on (8–13). This ultimately leads to the activation of TANK-binding kinase 1 (TBK1), which then phosphorylates IFN regulatory factor 3 (IRF3) at its C terminus. In turn, IRF3 dimerizes and translocates into nucleus (14). A dozen proteins have been reported to regulate this signaling pathway (15). In addition, the MAVS signalosome could activate the IκB kinase (IKK) complex and NF-κB. The transcription factors IRF3 and NF-κB synergistically induce the early production of type I IFNs and subsequent establishment of antiviral state (16, 17).

Laboratory of Molecular Cell Biology, Institute of Biochemistry and Cell Biology, Shanghai Institutes for Biological Sciences, Chinese Academy of Sciences, Shanghai 200031, China

[1]Y.H. and H.L. contributed equally to this work.

Received for publication July 18, 2011. Accepted for publication October 29, 2011.

This work was supported by National Natural Science Foundation of China Grant 31030021 and Ministry of Science and Technology of China Grants 2012CB910200, 2011CB910900, and 2010CB529703.

Address correspondence and reprint requests to Dr. Chen Wang, Shanghai Institutes for Biological Sciences, 320 Yue Yang Road, Shanghai 200031, China. E-mail address: cwang01@sibs.ac.cn

The online version of this article contains supplemental material.

Abbreviations used in this article: BMDM, bone marrow-derived macrophage; HA, hemagglutinin; IKK, IκB kinase; IRF3, IFN regulatory factor 3; ISG, IFN-stimulated gene; MOI, multiplicity of infection; NDV, Newcastle disease virus; poly(I:C), polyinosinic-polycytidylic acid; Q-PCR, quantitative PCR; SeV, Sendai virus; siRNA, small interfering RNA; TBK1, TANK-binding kinase 1; Tom, translocase of outer membrane; TRADD, TNFR-associated death domain protein; TRAF, TNFR-associated factor; VSV, vesicular stomatitis virus; WT, wild-type.



www.jimmunol.org/cgi/doi/10.4049/jimmunol.1102079

MAVS localizes on the mitochondrial outer membrane via its C-terminal *trans*-membrane domain, and this unique localization is essential for triggering the downstream antiviral cascades. As the core scaffold adaptor, MAVS interacts with multiple proteins, including TRADD, Fas-associated protein with death domain, caspase-8/9, TRAF2/3/6, IKKε, translocase of outer membrane (Tom) 70, receptor-interacting protein, stimulator of IFN genes, and NLR family member X1 (13, 18–24).

Mouse knockout analysis reveals the essential role of TRAF3 for the IRF3 activation during virus infection (12). Consistently, patients harboring a spontaneous mutation of the TRAF3 allele are defective in the activation of NF-κB and the induction of IFNs, due to TRAF3 deficiency (25). It is proposed that TRAF3 functions immediately downstream of the MAVS. A TRAF-binding motif (455-PEENEY-460) has been identified in MAVS. Mutating this motif abolishes the ability of MAVS to interact with TRAF3 and cripples the MAVS-dependent IFN production (26). Conversely, mutating the Y440 and Q442 of TRAF3 attenuates its binding to MAVS (19, 27). Interestingly, the E3 ligase Triad3A could catalyze the $Lys^{48}$-linked polyubiquitination of TRAF3 and downregulate TRAF3 (28). It remains to address how the MAVS signalosome is assembled temporally and spatially, and what specific roles these proteins play in innate immunity.

In the current study, we characterize ubiquitously expressed transcript (UXT)-V1 as an important modulator for antiviral signaling. UXT-V1 represents a novel integral component of the MAVS signalosome on mitochondria, essential for targeting TRAF3 and TRADD onto mitochondria following virus infection.

## Materials and Methods

### *Reagents*

The anti-UXT mAb was provided by W. Krek (Swiss Federal Institute of Technology Zurich, Switzerland). The following Abs were used for Western blot or immunoprecipitation: Sp1 (S9809; Sigma-Aldrich), α-tubulin (T9026; Sigma-Aldrich), β-actin (A5316; Sigma-Aldrich), normal mouse IgG (sc-2025; Santa Cruz Biotechnology), normal rabbit IgG (sc-2027; Santa Cruz Biotechnology), hemagglutinin (HA; sc-7392, Santa Cruz Biotechnology; ab9110, Abcam), Flag (F1804; Sigma-Aldrich), TRAF3 (sc-1828; Santa Cruz Biotechnology), TRAF2 (sc-876 and sc-7346; Santa Cruz Biotechnology), TRAF6 (sc-8409; Santa Cruz Biotechnology), TRADD (sc-46653; Santa Cruz Biotechnology), Tom20 (11802-1-AP; Proteintech), caspase-3 (9662; Cell Signaling), cleaved caspase-3 (9661; Cell Signaling), and MAVS (3993; Cell Signaling). Polyinosinic-polycytidylic acid [poly(I:C)] was purchased from GE Healthcare and was used at 10 mg/ml.

TNF-α was obtained from R&D Systems. LPS was purchased from Invitrogen. Vesicular stomatitis virus (VSV) and Newcastle disease virus (NDV)-GFP were provided by H. Shu (Wuhan University) and Z. Bu (Chinese Academy of Agricultural Sciences), respectively.

### *Cell culture and manipulation of primary cells*

HeLa, HEK293, HEK293T, NIH3T3, and RAW264.7 cell lines were obtained from the American Type Culture Collection and cultured according to the manufacturer's instructions. Bone marrow-derived macrophages (BMDMs) were obtained, as described previously (29). BMDMs were harvested after ~6~10 d and recultured in 12-well plates for small interfering RNA (siRNA) transfection using lipofectamine 2000 (Invitrogen) and further experiments.

### *Plasmids, siRNA oligos, and cell transfection*

Human or mouse UXT-V1 and TRAF3 cDNAs were amplified by RT-PCR from total RNA of HEK293T cells or NIH3T3 cells, respectively. The siRNA oligos against UXT-V1 were synthesized by GenePharma (human UXT-V1 siRNA, 5′-GGC UGA ACC UCC AGC UUG ATT-3′; mouse UXT-V1 siRNA, 5′-GAA GUU UAA AUA GAG CGC UTT-3′). The cells were transfected with siRNA oligos using Lipofectamine 2000, and were incubated for 48 h before further analysis. In the rescue assay, the plasmids were introduced into cells after these cells were transfected with siRNAs for 24 h, and then were maintained for another 24 h before further analysis.

### *Nuclear extraction*

Nuclear extractions of HEK293 cells were prepared, as described previously (30).

### *Western blot and immunoprecipitation*

Cell pellet was collected and resuspended in radioimmunoprecipitation assay buffer (50 mM Tris-HCl [pH 7.4], 150 mM NaCl, 1 mM EDTA, 0.5% Nonidet P-40, 0.25% Na-deoxycholate, 1 mM $Na_3VO_4$, 0.1 mM PMSF, Roche complete protease inhibitor set) for immunoprecipitation, or in RIPA buffer plus 0.1% SDS for Western blot. The resuspended cell pellet was vortexed for 20 s, then incubated on ice for 20 min, and

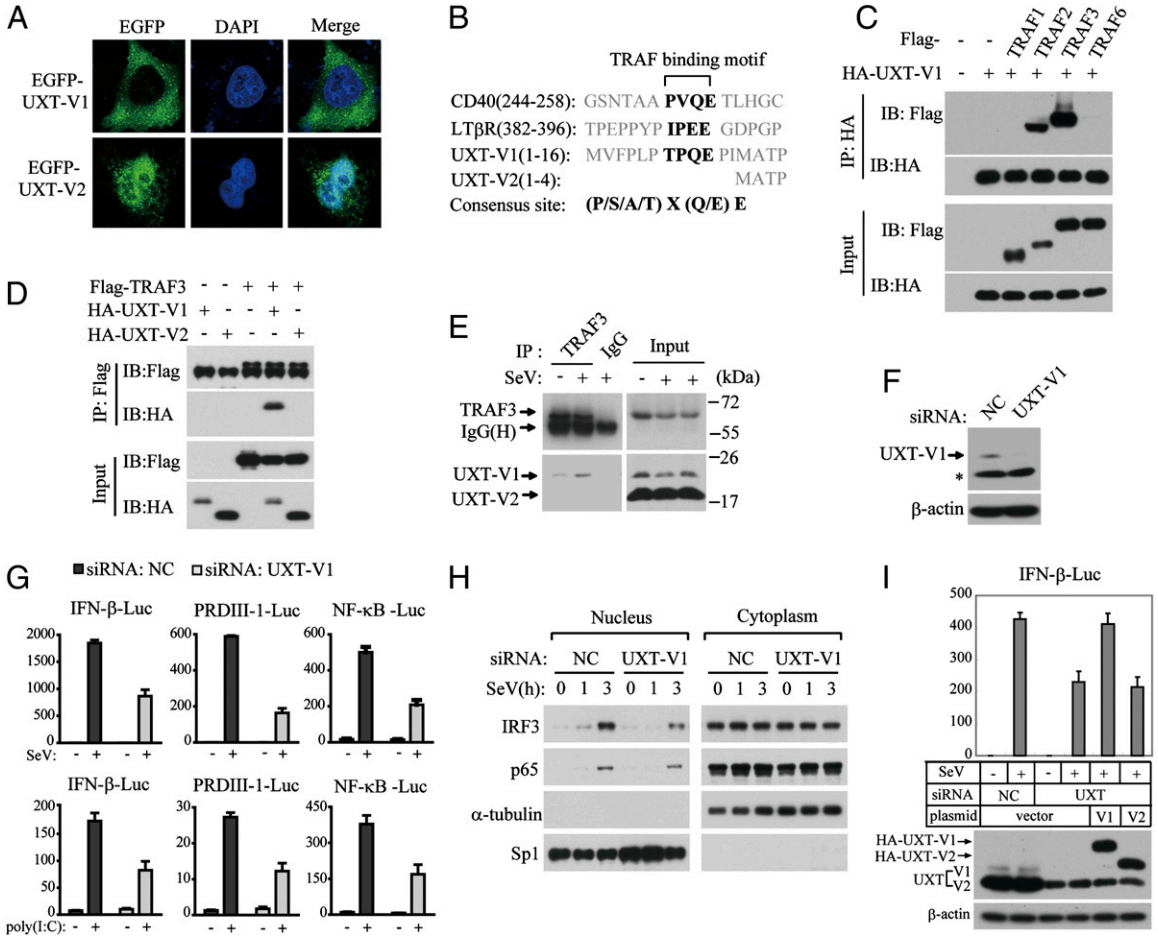


**FIGURE 1.** UXT-V1 binds to TRAF3 and is required for the activation of IRF3 and NF-κB. *A*, Confocal microscopy analysis of HeLa cells transfected with UXT-V1 or UXT-V2, with enhanced GFP tagged at the N terminus. Images were captured using a confocal microscope with a ×63 oil objective. *B*, Sequence alignment of the TRAF-binding motifs in CD40, LTβR, and UXT-V1. *C*, Flag-tagged TRAF1/2/3/6 was cotransfected into HEK293T cells along with HA-UXT-V1. Cell lysates were subjected to an immunoprecipitation assay using anti-HA Ab (source: rabbit), followed by Western blot analysis using anti-HA (source: mouse) Ab and anti-Flag Ab (source: mouse). *D*, Flag-TRAF3 was cotransfected into HEK293T cells along with HA-UXT-V1 or HA-UXT-V2. Cell lysates were subjected to an immunoprecipitation assay using anti-Flag Ab, followed by Western blot analysis using anti-HA Ab and anti-Flag Ab. *E*, HEK293 cell lysates were immunoprecipitated with anti-TRAF3 Ab or control IgG, followed by Western blot analysis with anti-TRAF3 Ab and anti-UXT Ab. *F*, HEK293 cells were transfected with nonspecific control (NC) or UXT-V1 siRNAs for 48 h, and then cell lysates were immunoblotted with anti-UXT Ab or anti–β-actin Ab, respectively. *UXT-V2. *G*, The indicated siRNAs were transfected into HEK293 cells together with IFN-β-Luc, PRDIII-1-Luc, or NF-κB-Luc reporter plasmids. Twenty-four hours after transfection, cells were infected with SeV (*upper*), or were transfected with poly(I:C) (*lower*). The luciferase assay was performed 12 h poststimulation. Data are presented as means ± SD ($n$ = 3). *H*, Control or UXT-V1 knocked down HEK293 cells were treated with SeV at the indicated time, and then cytoplasmic and nuclear fractions were extracted for immunoblot of IRF3, p65, Sp1, and α-tubulin. The levels of Sp1 and α-tubulin were applied to indicate accuracy of fractionation. *I*, HEK293 cells were transfected with UXT-V1 siRNA, and then rescued with pCDNA3 vector, UXT-V1, or UXT-V2 expression plasmids, respectively. Twelve hours after SeV infection, luciferase assay was performed, followed by Western blot analysis using anti-UXT Ab.

centrifuged at 20,000 × *g* for 15 min. The supernatants were collected for Western blot analysis or immunoprecipitation.

For immunoprecipitation, cell lysates were precleared with Protein A/G Plus-Agarose (Santa Cruz Biotechnology) at 4°C for 2 h, and then Ab or control IgG was added and incubated overnight. The next day, the cell lysates were incubated for another 2 h because the Protein A/G Plus-Agarose beads were added. The beads were washed with TBS buffer containing 0.5% Nonidet P-40; then the beads were boiled using 1× SDS loading buffer, and the supernatants were prepared for Western blot analysis.

### *Confocal microscopy*

Twenty-four hours after being transfected with enhanced GFP-tagged plasmids, cells cultured on coverslips were fixed with 4% paraformaldehyde (Sigma-Aldrich), and nuclei were stained with DAPI (Sigma-Aldrich). Slides were mounted by Aqua-Poly/Mount coverslipping medium (Polysciences). Images were captured using a confocal microscopy (TCS SP2 AOBS; Leica) with an original magnification ×63 NA 1.4 oil objective.

### *Flow cytometry*

Twelve hours after NDV-GVP infection, HEK293 cells were collected and washed by PBS buffer. Then the GFP-positive cells were measured using FACSCalibur (BD Biosciences), and the data were analyzed with Flowjo software.

### *Quantitative PCR*

Total cellular RNA was isolated with TRIzol (Invitrogen), according to the manufacturer's instructions. Reverse transcription of purified RNA was performed using oligo(dT) primer. The quantification of gene transcripts was performed by real-time PCR using SYBR Green PCR mix (Applied Biosystems). All values were normalized to the level of β-actin mRNA. The primers used were as follows. Primers for human: β-actin, sense (5′-AAA GAC CTG TAC GCC AAC AC-3′) and antisense (5′-GTC ATA CTC CTG CTT GCT GAT-3′); IFN-β, sense (5′-ATT GCC TCA AGG ACA GGA TG-3′) and antisense (5′-GGC CTT CAG GTA ATG CAG AA-3′); IL-8, sense (5′-AGG TGC AGT TTT GCC AAG GA-3′) and antisense (5′-TTT CTG TGT TGG CGC AGT GT-3′); and IFN-stimulated gene (ISG)

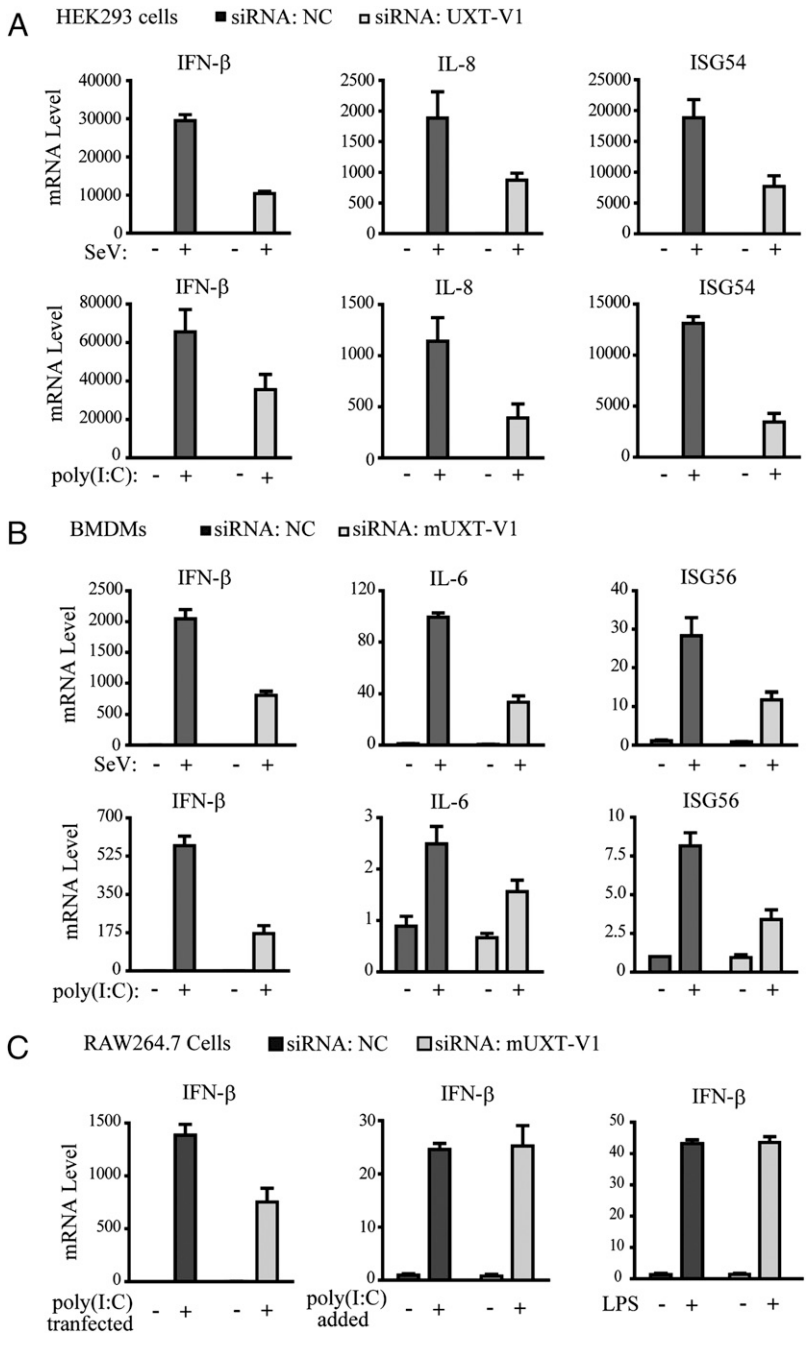


**FIGURE 2.** UXT-V1 modulates host antiviral responses. HEK293 cells (*A*) or BMDMs (*B*) were transfected with indicated siRNA and challenged by SeV infection (*upper*) or poly(I:C) transfection (*lower*) for 6 h. Then induction of indicated mRNAs was measured by Q-PCR. Data are presented as means ± SD ($n = 3$). *C*, NC or mUXT-V1 siRNAs were transfected into RAW264.7 cells, respectively. Forty-eight hours after transfection, cells were stimulated with poly(I:C) (2 μg/ml, transfected), poly(I:C) (50 μg/ml, added to the culture medium), and LPS (100 ng/ml). Then the induction of IFN-β mRNA was measured by Q-PCR. Data are presented as means ± SD ($n = 3$).

54, sense (5′-TGC AAC CTA CTG GCC TAT CTA-3′) and antisense (5′-CAG GTG ACC AGA CTT CTG ATT-3′). Primers for mouse: β-actin, sense (5′-AGA CCT CTA TGC CAA CAC AG-3′) and antisense (5′-TCG TAC TCC TGC TTG CTG AT-3′); IFN-β, sense (5′-AGA TCA ACC TCA CCT ACA GG-3′) and antisense (5′-TCA GAA ACA CTG TCT GCT GG-3′); IL-6, sense (5′-GAG AGG AGA CTT CAC AGA GG-3′) and antisense (5′-GTA CTC CAG AAG ACC AGA GG-3′); and ISG56, sense (5′-AGT GCA GGC AGA AAT TCA CC-3′) and antisense (5′-AGC AGT CAG TAG TTT CCT CC-3′).

### *Subcellular fractionation*

HEK293 cells were washed with cold PBS and lysed by Dounce homogenizer in homogenization buffer (210 mM sucrose, 70 mM mannitol, 1 mM EDTA, 1 mM EGTA, 1.5 mM $MgCl_2$, 10 mM HEPES [pH 7.2]). The homogenate was centrifuged at 500 × *g* for 10 min, and the pellet was discarded as crude nuclei. The supernatant was centrifuged at 5000 × *g* for 10 min to precipitate crude mitochondria; then the supernatants were collected as cytosolic fraction, and the precipitate was lysed by RIPA buffer as mitochondria fraction.

### *Virus manipulation*

Viral infection was performed when 80% cell confluence was reached. Then, culture medium was replaced by serum-free DMEM, and Sendai virus (SeV), VSV, or NDV-GFP was added to the media at multiplicity of infection (MOI) of 0.2–1, according to specific experiments. After 1 h, the medium was removed and the cells were fed with DMEM containing 10% FBS.

## Results

### *UXT-V1 binds to TRAF3 and is required for the activation of IRF3 and NF-κB*

There are two mRNA splicing isoforms of UXT in cells, which we name as UXT-V1 and UXT-V2, respectively. Previously, we characterized UXT-V2 as a novel transcriptional cofactor to regulate NF-κB in the nucleus (31). However, it came to our attention that those two isoforms represented different subcellular localization. Whereas UXT-V2 predominantly resided in nucleus, UXT-V1 was reproducibly found to localize in cytoplasm (Fig. 1*A*), which suggested that UXT-V1 could perform different functions from that of UXT-V2. Structurally, UXT-V1 (169 aa) harbored 12 more amino acids on its N terminus than UXT-V2 (157 aa). Through the Bioinformatics method, a potential TRAF-binding motif –TPQE was identified in the N terminus of UXT-V1. This consensus sequence, (P/S/A/T) X (Q/E) E, was previously identified in TRAF-binding proteins, such as CD40 and LTβR (Fig. 1*B*) (32–35). So we explored the possible interaction between UXT-V1 and TRAF family proteins. Interestingly, UXT-V1 could bind strongly to TRAF2 and TRAF3 (Fig. 1*C*). Our recent study explored the function of the UXT-V1–TRAF2 interaction and revealed that UXT-V1 was an important regulator of TNF-induced apoptosis (30).

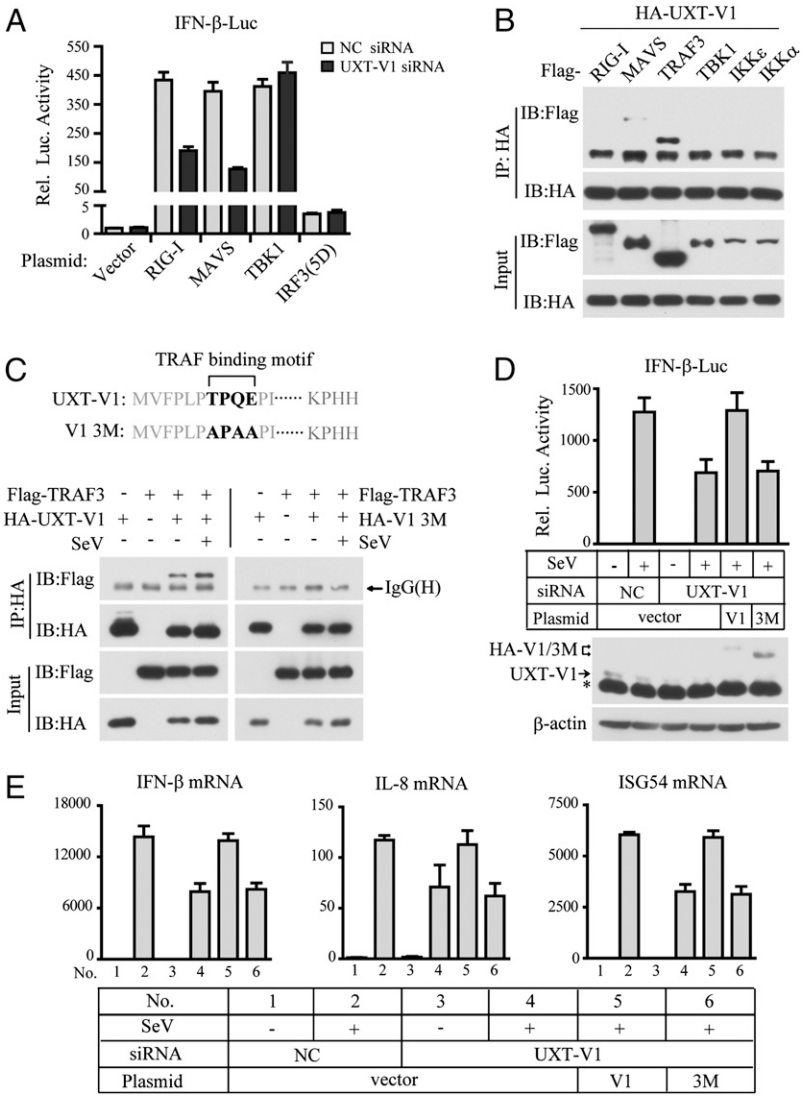


**FIGURE 3.** The TRAF-binding motif is essential for UXT-V1's antiviral function. *A*, Control or UXT-V1 siRNAs were transfected into HEK293 cells along with IFN-β-Luc reporters. Twenty-four hours after transfection, the indicated expressing plasmids were introduced into these cells, respectively. After another 24 h, the luciferase assay was performed. *B*, The indicated plasmids with Flag tagged were respectively transfected into HEK293T cells along with HA-UXT-V1, and then cell lysates were immunoprecipitated with anti-HA Ab, followed by Western blot analysis with anti-Flag Ab and anti-HA Ab. *C*, *Upper*, The mutation sites of UXT-V1(3M) in reference to UXT-V1(WT). *Lower*, The indicated combination of plasmids was introduced into HEK293T cells, followed by immunoprecipitation and Western blot assays, as described in *B*. *D*, HEK293 cells were transfected with UXT-V1 siRNA, and then rescued with pCDNA3 vector, UXT-V1(WT), or UXT-V1(3M) expression plasmids, respectively. Twelve hours after SeV infection, luciferase assay was performed, followed by Western blot analysis using anti-UXT Ab. *UXT-V2. *E*, The similar rescue assays were processed, as described in *D*, and then induction of IFN-β, IL-8, and ISG54 mRNAs was measured by Q-PCR. Data in *A*, *D*, and *E* are presented as means ± SD ($n$ = 3).

In the current study, we went on to investigate the potential function of the UXT-V1–TRAF3 interaction in innate immunity. To further verify this interaction, an exogenous immunoprecipitation assay was performed in HEK293T cells. Apparently, UXT-V1 could be coimmunoprecipitated with Flag-TRAF3, whereas UXT-V2 could not (Fig. 1*D*). The endogenous interaction between UXT-V1 and TRAF3 was also confirmed, and this interaction was enhanced upon SeV infection (Fig. 1*E*), indicating that UXT-V1 is a novel TRAF3-binding protein.

Given the essential role of TRAF3 in innate immunity, we screened out a siRNA that could specifically knock down UXT-V1 without affecting the UXT-V2 expression (Fig. 1*F*). To explore the potential function of UXT-V1 in antiviral signaling, it was observed that knockdown of UXT-V1 apparently inhibited the activation of the IFN-β luciferase reporter, stimulated by either SeV infection or poly(I:C) transfection (Fig. 1*G*). Consistently, the induction of κB (responsive to NF-κB) or PRDIII-1 (responsive to IRF3) luciferase reporters was attenuated in the absence of endogenous UXT-V1 (Fig. 1*G*). In addition, knockdown of UXT-V1 restrained the nuclear translocation of both NF-κB and IRF3 upon virus infection (Fig. 1*H*). Collectively, these data suggest that UXT-V1 could play some role in the activation of IRF3 and NF-κB.

Furthermore, we performed a rescue assay to distinguish the functions of UXT-V1 and UXT-V2. We knocked down both UXT-V1 and UXT-V2, and then reintroduced HA-UXT-V1– or HA-UXT-V2–expressing plasmids into HEK293 cells, respectively. Clearly, UXT-V1 could rescue the activation of IFN-β luciferase reporter upon SeV infection, but UXT-V2 could not do so (Fig. 1*I*). This indicates UXT-V2 does not regulate the antiviral signaling pathway.

### *UXT-V1 regulates the induction of antiviral factors*

To further substantiate the function of UXT-V1, we measured the expression of the antiviral genes via quantitative PCR (Q-PCR), after stimulating HEK293 cells by SeV infection or poly(I:C) transfection. Notably, the induction of IFN-β, IL-8 (NF-κB–responsive gene), and ISG54 (IRF3-responsive gene) was attenuated when knocking down UXT-V1 (Fig. 2*A*). To make it more physiologically relevant, knockdown of UXT-V1 markedly impaired the induction of IFN-β, IL-6, and ISG56 in BMDMs, after stimulating by SeV infection or poly(I:C) transfection (Fig. 2*B*). These data indicate that UXT-V1 is a positive modulator of RIG-I–mediated IRF3 and NF-κB antiviral signaling.

Given that UXT-V1 regulates TNF-induced apoptosis, we wondered whether UXT-V1 could modulate SeV-induced apoptosis. As shown in Supplemental Fig. 1, cell apoptosis did not occur until 16 h after Sendai virus infection, whereas the IFNs were robustly induced within 6 h (Fig. 2*A*, 2*B*). Importantly, knockdown of UXT-V1 had no effect on SeV-induced apoptosis (Supplemental Fig. 1).

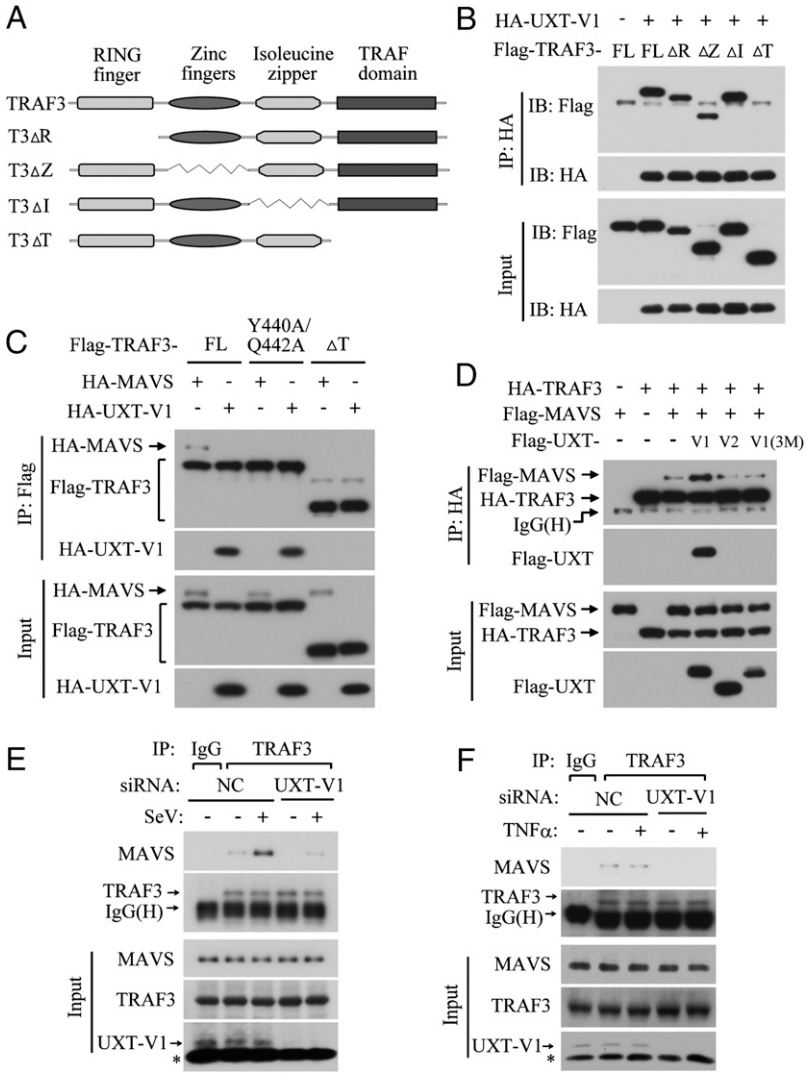


**FIGURE 4.** UXT-V1 facilitates the interaction between TRAF3 and MAVS. *A*, Schematic diagram of TRAF3 and its truncation mutants. *B*, Flag-TRAF3 or its truncation mutants were transfected into HEK293T cells along with HA-UXT-V1. Then cell lysates were immunoprecipitated with anti-HA Ab, followed by Western blot analysis with anti-Flag Ab and anti-HA Ab. *C* and *D*, HEK293T cells were transfected with the indicated combination of plasmids. Flag (*C*) or HA (*D*) immunoprecipitation and Western blot assays were performed, as previously described. *E* and *F*, HEK293 cells transfected with indicated siRNAs were treated with SeV (*E*) or TNF-α (*F*) for 1 h. Cell lysates were immunoprecipitated by anti-TRAF3 Ab, followed by Western blot analysis with anti-TRAF3, anti-MAVS, or anti-UXT Abs, respectively. FL, full length.

Furthermore, we probed whether UXT-V1 could affect other signaling pathways in innate immunity. Apparently, knockdown of UXT-V1 did not influence the IFN-β production stimulated by extracellular poly(I:C) or LPS in RAW264.7 cells (Fig. 2*C*). Neither could UXT-V1 influence the induction of IFN-β in 293-TLR3 cells upon extracellular poly(I:C) stimulation (Supplemental Fig. 2). These data indicate that UXT-V1 has no effect for TLR3 or TLR4 signaling. Notably, knockdown of UXT-V1 markedly impairs the RIG-I signaling, which is modulated by TRAF3 (12).

### *The TRAF-binding motif is essential for UXT-V1's antiviral function*

To delineate the topology of UXT-V1 in the RIG-I/MAVS/TBK1/IRF3 signaling pathway, we individually introduced the expressing plasmids of these four proteins into control cells or UXT-V1 knockdown cells for activating IFN-β luciferase reporter. Notably, knockdown of UXT-V1 attenuated the activation of IFN-β reporter in response to RIG-I or MAVS, but did not in response to TBK1 or IRF3-5D (Fig. 3*A*). Furthermore, UXT-V1 marginally bound to MAVS, and had no obvious interaction with RIG-I, TBK1, IKKε, or IKKα, although UXT-V1 interacted strongly with TRAF3 (Fig. 3*B*). This indicates that UXT-V1 acts downstream of RIG-I and MAVS and upstream of TBK1 and IRF3.

We went on to address the functional significance of the interaction between UXT-V1 and TRAF3. So, UXT-V1(3M) was generated, in which threonine (T), glutamine (Q), and glutamic acid (E) were all mutated to glycine (A) at residues 7, 9, and 10, respectively (Fig. 3*C*, *upper*). Interestingly, UXT-V1(3M) was deprived of the ability to interact with TRAF3 (Fig. 3*C*, *lower*), confirming that the N terminus of UXT-V1 was an authentic TRAF-binding motif toward TRAF3.

Then, the genetic rescue assays were performed in cells that had the endogenous UXT-V1 knocked down. As expected, wild-type (WT) UXT-V1 could significantly rescue the activation of IFN-β luciferase reporter stimulated by SeV infection. Notably, UXT-V1(3M) could not do so (Fig. 3*D*). Consistently, SeV-stimulated induction of the IFN-β, IL-8, or ISG54 was restored in the UXT-V1 knockdown cells, by introducing WT UXT-V1, but not by UXT-V1(3M) (Fig. 3*E*). Collectively, these data indicate that the TRAF-binding motif is essential for UXT-V1's antiviral function.

### *UXT-V1 facilitates the interaction between TRAF3 and MAVS*

To map the binding domain, we constructed four truncation mutants of TRAF3 (Fig. 4*A*). These truncation mutants were respectively transfected into HEK293T cells along with UXT-V1. As shown in Fig. 4*B*, the truncation mutant lacking the TRAF domain (△T) failed to interact with UXT-V1, indicating that the TRAF domain of TRAF3 mediates its interaction with UXT-V1. Interestingly, a recent study also characterized that the TRAF domain was responsible for binding MAVS. In particular, two amino acids, Y440 and Q442, in this TRAF domain were critical for TRAF3 to interact with MAVS (19, 26). So, we tested whether these two amino acids were also critical for TRAF3 to bind UXT-V1. Notably, the TRAF3 (Y440A/Q442A) could, as well as the TRAF3 (WT), interact with UXT-V1 (Fig. 4*C*). Consistently, TRAF3 (△T) could interact with neither MAVS nor UXT-V1 (Fig. 4*C*). Thus, UXT-V1 and MAVS target topologically different sites in the TRAF domain of TRAF3.

To probe the relationship among UXT-V1, TRAF3, and MAVS, the immunoprecipitation assay was performed and revealed that UXT-V1 could markedly potentiate the interaction between TRAF3 and MAVS, whereas UXT-V1(3M) or UXT-V2 failed to do so (Fig. 4*D*). Importantly, knockdown of UXT-V1 apparently attenuated the endogenous interaction between TRAF3 and MAVS, indicating that UXT-V1 promotes the formation of MAVS–TRAF3 complex following virus infection (Fig. 4*E*). In contrast, the MAVS and TRAF3 interaction was not modulated by the TNF-α stimulation (Fig. 4*F*). In addition, knockdown of UXT-V1 had no effect on the MAVS–TRAF6 interaction (Supplemental Fig. 3*A*), and there was no detectable interaction between TRAF2 and MAVS under the stimulation of TNF-α or SeV (Supplemental Fig. 3*B*). These data indicate that UXT-V1 regulates MAVS antiviral signaling by targeting TRAF3.

### *UXT-V1 facilitates the recruitment of TRAF3 and TRADD onto mitochondria*

Because MAVS is localized on the outer membrane of mitochondria, it is intriguing how TRAF3 and TRADD are recruited onto the MAVS signalosome. Subcellular fractionation was employed to monitor the locations of these proteins. In resting cells, TRAF3 or TRADD predominantly resided in the cytosolic fraction.

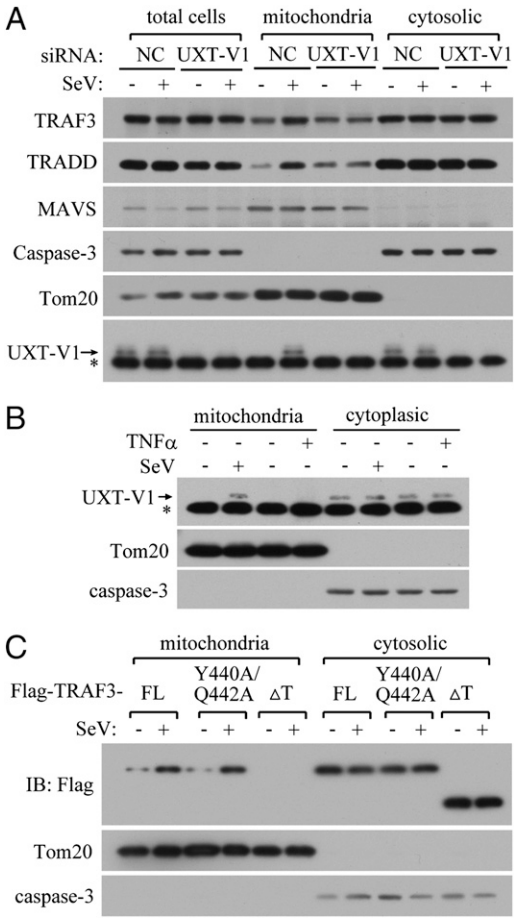


**FIGURE 5.** UXT-V1 facilitates the recruitment of TRAF3 and TRADD to mitochondria. *A*, HEK293 cells transfected with control or UXT-V1 siRNAs were stimulated with or without SeV for 1 h, and then the total cells and cytosolic and mitochondrial fractions were extracted for immunoblot of TRAF3, TRADD, MAVS, caspase-3, Tom20, and UXT-V1. The levels of caspase-3 and Tom20 were applied to indicate accuracy of fractionation. *UXT-V2. *B*, HEK293 cells were stimulated with SeV or TNF-α for 1 h, and then the cytosolic and mitochondrial fractions were extracted for immunoblot of caspase-3, Tom20, and UXT-V1. *C*, The indicated plasmids were introduced into HEK293 cells. One hour after SeV infected, subcellular fractionation assay was performed and the corresponding fractions were subjected to Western blot assay of Flag, caspase-3, and Tom20.

However, a tiny portion of them could constitutively be detected in the mitochondrial fraction, although this could also be due to cross-contamination of subcellular fractions. Notably, mitochondria-associated TRAF3 and TRADD were markedly increased following SeV treatment (Fig. 5*A*). More importantly, this phenomenon was abolished when silencing the endogenous UXT-V1 expression. In contrast, UXT-V1 apparently did not influence the presence of MAVS on mitochondria (Fig. 5*A*), suggesting that UXT-V1 modulates MAVS signalosome assemblage. In addition, UXT-V1 was present in the mitochondrial fraction upon SeV stimulation, but not upon TNF-α stimulation (Fig. 5*B*). This indicates that UXT-V1 is a novel component of the MAVS signalosome on mitochondria.

To further test this possibility, the TRAF3 (WT), TRAF3 (Y440A/Q442A), and TRAF3 (△T) were respectively introduced into HEK293 cells, stimulated or not by SeV, followed by subcellular fractionation. Despite lacking the ability to bind MAVS, TRAF3 (Y440A/Q442A) could be recruited onto mitochondria, as well as TRAF3 (WT), upon SeV infection. However, TRAF3 (△T), which could interact with neither MAVS nor UXT-V1, failed to be recruited onto mitochondria (Fig. 5*C*). Taken together, these data indicate that UXT-V1 facilitates the recruitment of TRAF3 to mitochondria.

### *UXT-V1 modulates host antiviral responses*

Finally, we assessed the role of UXT-V1 in virus restriction. Crystal violet staining revealed that knockdown of UXT-V1 made cells more sensitive to VSV infection (Fig. 6*A*). In addition, the titers of VSV were analyzed by standard plaque assay. Knockdown of UXT-V1 resulted in ~3-fold increase in virus titer as compared with the controls (Fig. 6*B*). We also investigated whether UXT-V1 modulated virus replication, by challenging cells with NDV-GFP. Consistently, NDV-GFP infection increased when knocking down UXT-V1 (Fig. 6*C*), and a 10-fold increase of NDV-GFP–positive cells was determined by flow cytometry assay (Fig. 6*D*). Taken together, these data demonstrate that UXT-V1 positively modulates innate antiviral responses.

## Discussion

UXT is widely present in human and mouse tissues. Bioinformatics analysis reveals two isoforms of UXT, namely UXT-V1 and UXT-V2. Previous investigations characterize UXT-V2 to function in the nucleus. For example, UXT-V2 is suggested to interact with the N terminus of the androgen receptor and regulate androgen-responsive genes (36). UXT-V2 is also implicated as a component of the centrosome (37). Our recent study uncovers UXT-V2 to positively modulate the NF-κB transcriptional enhanceosome. Unexpectedly, we observe that UXT-V1 expresses almost exclusively in the cytoplasm, and the functional characterization of UXT-V1 has not been determined (30).

MAVS signalosome is an emerging antiviral protein complex on mitochondria. Recent studies have characterized several proteins important for this antiviral signaling. Current research aims to understand the MAVS complex protein composition, temporal and spatial dynamics, and mechanism of signal transduction. Intriguingly, MAVS forms prion-like aggregates on mitochondria to activate antiviral innate immune response (38). In this study, we have identified UXT-V1 is a novel component of the MAVS signalosome, and it is critical for the virus-induced activation of NF-κB and IRF3. Thus, UXT-V1 represents a novel integral component of the MAVS signalosome on mitochondria, mediating the innate antiviral signal transduction.

MAVS per se localizes on the outer membrane of mitochondria via its C-terminal transmembrane domain. In resting cells, most of the proteins in the MAVS signalosome reside in cytosol, including TRAF3 and TRADD. Upon virus infection, these proteins are proposed to quickly aggregate with MAVS on mitochondria (23, 28). Thus, a critical missing link exists as to how MAVS relays signals to these cytosolic proteins. A recent study suggested that K63 polyubiquitination of MAVS could serve as a signal for the assemblage of the protein complex (39). By subcellular fractionation assay, we demonstrate the specific translocation of TRAF3/TRADD onto mitochondria upon virus infection. It remains unknown whether TRAF3/TRADD could bind to the polyubiquitin chain.

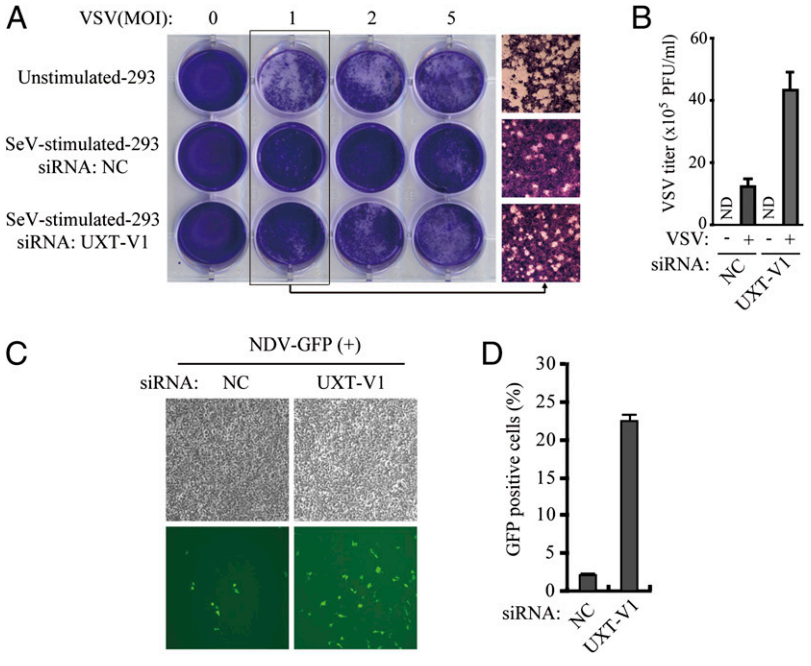


**FIGURE 6.** UXT-V1 modulates host antiviral responses. *A*, HEK293 cells were transfected with indicated siRNA and then treated with SeV. Equal volumes of culture supernatants from these treatments were applied to fresh HEK293 cells, followed by VSV infection at the indicated MOI. The proliferation of cells was determined by crystal violet staining (*left*). The viral plaques (MOI = 1) were observed by amplificatory microscopy (*right*, ×8 objective). *B*, The titers of VSV in *A* were determined by standard plaque assay. *C*, NDV-GFP replication in HEK293 cells transfected with control or UXT-V1 siRNAs was visualized by fluorescence microscopy (×20 objective). *D*, GFP-positive cells in *C* were quantified by flow cytometry assay. Data in *B* and *D* are presented as means ± SD ($n$ = 3).

TRAF3 is essential for both RIG-I/MDA5 and TLR signaling during virus infection. A spontaneous mutation of TRAF3 (R118W) in humans leads to the impairment of TLR3-dependent induction of IFN and the susceptibility to HSV-1. The generation of TRAF3$^{-/-}$ BMDMs establishes that TRAF3 functions as a bridge between MAVS and the downstream TBK1/IKKε. The C-terminal 455-PEENEY-460 TRAF-binding motif of MAVS is critical for recruiting TRAF3. In addition, Triad3A could target TRAF3 for Lys$^{48}$-linked ubiquitin-mediated degradation, and negatively regulate the RIG-I/MAVS signals. Two amino acids in the TRAF domain of TRAF3, Y440 and Q442, are reported to be pivotal for TRAF3 to bind MAVS (19, 26). However, the data presented show that the two amino acids, Y440 and Q442, are dispensable for TRAF3 to bind UXT-V1.

In this study, we observed that the translocation of TRAF3/TRADD to mitochondria is significantly blocked when knocking down UXT-V1. Notably, the N-terminal TRAF-binding motif of UXT-V1 binds to the C-terminal TRAF domain of TRAF3. Although MAVS also binds to the C-terminal TRAF domain of TRAF3, mutational analysis in this study revealed that UXT-V1 and MAVS target topologically different sites in the TRAF domain of TRAF3. We speculate that UXT-V1 serves to facilitate the interaction between TRAF3 and MAVS, thus modulating the strength and duration of the action of the MAVS signalosome.

Structural modeling predicts that UXT-V1 is a α-class prefoldin family protein (40). Most members of this family are small molecular mass proteins (14–23 kDa) with coiled-coil structures. Yeast and human prefoldins 1–6 are implicated as a new type of molecular chaperone (41). It will be intriguing to explore whether UXT-V1 functions as a unique molecular chaperone for targeting TRAF3 to MAVS on mitochondria. Hopefully, future structural analysis will shed light on the topological relationship of the MAVS–TRAF3–UXT-V1 protein complex, revealing the mechanistic assemblage of the MAVS signalosome.

## Acknowledgments

We thank Drs. Wilhelm Krek (Eidgenössische Technische Hochschule Zürich) and Hongbing Shu (Wuhan University) for reagents.

## Disclosures

The authors have no financial conflicts of interest.

## References

1. Janeway, C. A., Jr. 1989. Approaching the asymptote? Evolution and revolution in immunology. *Cold Spring Harb. Symp. Quant. Biol.* 54: 1–13.
2. Medzhitov, R., and C. A. Janeway, Jr. 1998. Innate immune recognition and control of adaptive immune responses. *Semin. Immunol.* 10: 351–353.
3. Meylan, E., and J. Tschopp. 2006. Toll-like receptors and RNA helicases: two parallel ways to trigger antiviral responses. *Mol. Cell* 22: 561–569.
4. Uematsu, S., and S. Akira. 2006. Toll-like receptors and innate immunity. *J. Mol. Med.* 84: 712–725.
5. Yoneyama, M., and T. Fujita. 2008. Structural mechanism of RNA recognition by the RIG-I-like receptors. *Immunity* 29: 178–181.
6. Kawai, T., and S. Akira. 2008. Toll-like receptor and RIG-I-like receptor signaling. *Ann. N. Y. Acad. Sci.* 1143: 1–20.
7. Sun, L., S. Liu, and Z. J. Chen. 2010. SnapShot: pathways of antiviral innate immunity. *Cell* 140: 436–436.e2.
8. Seth, R. B., L. Sun, C. K. Ea, and Z. J. Chen. 2005. Identification and characterization of MAVS, a mitochondrial antiviral signaling protein that activates NF-kappaB and IRF 3. *Cell* 122: 669–682.
9. Kawai, T., K. Takahashi, S. Sato, C. Coban, H. Kumar, H. Kato, K. J. Ishii, O. Takeuchi, and S. Akira. 2005. IPS-1, an adaptor triggering RIG-I- and Mda5-mediated type I interferon induction. *Nat. Immunol.* 6: 981–988.
10. Meylan, E., J. Curran, K. Hofmann, D. Moradpour, M. Binder, R. Bartenschlager, and J. Tschopp. 2005. Cardif is an adaptor protein in the RIG-I antiviral pathway and is targeted by hepatitis C virus. *Nature* 437: 1167–1172.
11. Xu, L. G., Y. Y. Wang, K. J. Han, L. Y. Li, Z. Zhai, and H. B. Shu. 2005. VISA is an adapter protein required for virus-triggered IFN-beta signaling. *Mol. Cell* 19: 727–740.
12. Oganesyan, G., S. K. Saha, B. Guo, J. Q. He, A. Shahangian, B. Zarnegar, A. Perry, and G. Cheng. 2006. Critical role of TRAF3 in the Toll-like receptor-dependent and -independent antiviral response. *Nature* 439: 208–211.
13. Michallet, M. C., E. Meylan, M. A. Ermolaeva, J. Vazquez, M. Rebsamen, J. Curran, H. Poeck, M. Bscheider, G. Hartmann, M. König, et al. 2008. TRADD protein is an essential component of the RIG-like helicase antiviral pathway. *Immunity* 28: 651–661.
14. Honda, K., A. Takaoka, and T. Taniguchi. 2006. Type I interferon [corrected] gene induction by the interferon regulatory factor family of transcription factors. *Immunity* 25: 349–360.
15. Hiscott, J. 2007. Triggering the innate antiviral response through IRF-3 activation. *J. Biol. Chem.* 282: 15325–15329.
16. Yoneyama, M., and T. Fujita. 2010. Recognition of viral nucleic acids in innate immunity. *Rev. Med. Virol.* 20: 4–22.
17. Hiscott, J. 2007. Convergence of the NF-kappaB and IRF pathways in the regulation of the innate antiviral response. *Cytokine Growth Factor Rev.* 18: 483–490.
18. Balachandran, S., E. Thomas, and G. N. Barber. 2004. A FADD-dependent innate immune mechanism in mammalian cells. *Nature* 432: 401–405.
19. Saha, S. K., E. M. Pietras, J. Q. He, J. R. Kang, S. Y. Liu, G. Oganesyan, A. Shahangian, B. Zarnegar, T. L. Shiba, Y. Wang, and G. Cheng. 2006. Regulation of antiviral responses by a direct and specific interaction between TRAF3 and Cardif. *EMBO J.* 25: 3257–3263.
20. Ishikawa, H., and G. N. Barber. 2008. STING is an endoplasmic reticulum adaptor that facilitates innate immune signalling. *Nature* 455: 674–678.
21. Moore, C. B., D. T. Bergstralh, J. A. Duncan, Y. Lei, T. E. Morrison, A. G. Zimmermann, M. A. Accavitti-Loper, V. J. Madden, L. Sun, Z. Ye, et al. 2008. NLRX1 is a regulator of mitochondrial antiviral immunity. *Nature* 451: 573–577.
22. Liu, X. Y., B. Wei, H. X. Shi, Y. F. Shan, and C. Wang. 2010. Tom70 mediates activation of interferon regulatory factor 3 on mitochondria. *Cell Res.* 20: 994–1011.
23. Wang, C., X. Liu, and B. Wei. 2011. Mitochondrion: an emerging platform critical for host antiviral signaling. *Expert Opin. Ther. Targets* 15: 647–665.
24. Zhong, B., Y. Yang, S. Li, Y. Y. Wang, Y. Li, F. Diao, C. Lei, X. He, L. Zhang, P. Tien, and H. B. Shu. 2008. The adaptor protein MITA links virus-sensing receptors to IRF3 transcription factor activation. *Immunity* 29: 538–550.
25. Pérez de Diego, R., V. Sancho-Shimizu, L. Lorenzo, A. Puel, S. Plancoulaine, C. Picard, M. Herman, A. Cardon, A. Durandy, J. Bustamante, et al. 2010. Human TRAF3 adaptor molecule deficiency leads to impaired Toll-like receptor 3 response and susceptibility to herpes simplex encephalitis. *Immunity* 33: 400–411.
26. Paz, S., M. Vilasco, S. J. Werden, M. Arguello, D. Joseph-Pillai, T. Zhao, T. L. Nguyen, Q. Sun, E. F. Meurs, R. Lin, and J. Hiscott. 2011. A functional C-terminal TRAF3-binding site in MAVS participates in positive and negative regulation of the IFN antiviral response. *Cell Res.* 21: 895–910.
27. Ni, C. Z., G. Oganesyan, K. Welsh, X. Zhu, J. C. Reed, A. C. Satterthwait, G. Cheng, and K. R. Ely. 2004. Key molecular contacts promote recognition of the BAFF receptor by TNF receptor-associated factor 3: implications for intracellular signaling regulation. *J. Immunol.* 173: 7394–7400.
28. Nakhaei, P., T. Mesplede, M. Solis, Q. Sun, T. Zhao, L. Yang, T. H. Chuang, C. F. Ware, R. Lin, and J. Hiscott. 2009. The E3 ubiquitin ligase Triad3A negatively regulates the RIG-I/MAVS signaling pathway by targeting TRAF3 for degradation. *PLoS Pathog.* 5: e1000650.
29. Lou, X., S. Sun, W. Chen, Y. Zhou, Y. Huang, X. Liu, Y. Shan, and C. Wang. 2011. Negative feedback regulation of NF-κB action by CITED2 in the nucleus. *J. Immunol.* 186: 539–548.
30. Huang, Y., L. Chen, Y. Zhou, H. Liu, J. Yang, Z. Liu, and C. Wang. 2011. UXT-V1 protects cells against TNF-induced apoptosis through modulating complex II formation. *Mol. Biol. Cell* 22: 1389–1397.
31. Sun, S., Y. Tang, X. Lou, L. Zhu, K. Yang, B. Zhang, H. Shi, and C. Wang. 2007. UXT is a novel and essential cofactor in the NF-kappaB transcriptional enhanceosome. *J. Cell Biol.* 178: 231–244.
32. Ni, C. Z., K. Welsh, E. Leo, C. K. Chiou, H. Wu, J. C. Reed, and K. R. Ely. 2000. Molecular basis for CD40 signaling mediated by TRAF3. *Proc. Natl. Acad. Sci. USA* 97: 10395–10399.
33. Jabara, H., D. Laouini, E. Tsitsikov, E. Mizoguchi, A. Bhan, E. Castigli, F. Dedeoglu, V. Pivniouk, S. Brodeur, and R. Geha. 2002. The binding site for TRAF2 and TRAF3 but not for TRAF6 is essential for CD40-mediated immunoglobulin class switching. *Immunity* 17: 265–276.
34. Li, C., P. S. Norris, C. Z. Ni, M. L. Havert, E. M. Chiong, B. R. Tran, E. Cabezas, J. C. Reed, A. C. Satterthwait, C. F. Ware, and K. R. Ely. 2003. Structurally distinct recognition motifs in lymphotoxin-beta receptor and CD40 for tumor necrosis factor receptor-associated factor (TRAF)-mediated signaling. *J. Biol. Chem.* 278: 50523–50529.
35. Ely, K. R., R. Kodandapani, and S. Wu. 2007. Protein-protein interactions in TRAF3. *Adv. Exp. Med. Biol.* 597: 114–121.
36. Markus, S. M., S. S. Taneja, S. K. Logan, W. Li, S. Ha, A. B. Hittelman, I. Rogatsky, and M. J. Garabedian. 2002. Identification and characterization of ART-27, a novel coactivator for the androgen receptor N terminus. *Mol. Biol. Cell* 13: 670–682.
37. Zhao, H., Q. Wang, H. Zhang, Q. Liu, X. Du, M. Richter, and M. I. Greene. 2005. UXT is a novel centrosomal protein essential for cell viability. *Mol. Biol. Cell* 16: 5857–5865.
38. Hou, F., L. Sun, H. Zheng, B. Skaug, Q. X. Jiang, and Z. J. Chen. 2011. MAVS forms functional prion-like aggregates to activate and propagate antiviral innate immune response. *Cell* 146: 448–461.

39. You, F., H. Sun, X. Zhou, W. Sun, S. Liang, Z. Zhai, and Z. Jiang. 2009. PCBP2 mediates degradation of the adaptor MAVS via the HECT ubiquitin ligase AIP4. *Nat. Immunol.* 10: 1300–1308.
40. Gstaiger, M., B. Luke, D. Hess, E. J. Oakeley, C. Wirbelauer, M. Blondel, M. Vigneron, M. Peter, and W. Krek. 2003. Control of nutrient-sensitive transcription programs by the unconventional prefoldin URI. *Science* 302: 1208–1212.
41. Siegert, R., M. R. Leroux, C. Scheufler, F. U. Hartl, and I. Moarefi. 2000. Structure of the molecular chaperone prefoldin: unique interaction of multiple coiled coil tentacles with unfolded proteins. *Cell* 103: 621–632.